

# Weak Adversarial Neural Pushforward Method for the McKean–Vlasov / Mean-Field Fokker–Planck Equation

Andrew Qing He\*      Wei Cai\*

March 18, 2026

## Abstract

We extend the Weak Adversarial Neural Pushforward Method (WANPM) [1] to the McKean–Vlasov mean-field Fokker–Planck equation. For the quadratic interaction kernel, the mean-field nonlinearity reduces to a batch sample mean, requiring no secondary sampling. We focus on the stationary problem, identifying key training subtleties: gradient flow through the self-consistent mean estimate is essential for uniqueness, and adversarial test function frequencies must be initialized at a sufficiently large scale to avoid spurious minimizers. A numerical benchmark on the 1D linear McKean–Vlasov equation confirms accurate recovery of the exact Gaussian stationary distribution.

**Keywords:** McKean–Vlasov equation, mean-field Fokker–Planck, neural pushforward map, weak adversarial network, plane-wave test functions, granular media, interacting particle systems.

## Contents

<b>1</b>	<b>Introduction</b>	<b>2</b>
<b>2</b>	<b>The McKean–Vlasov Equation</b>	<b>3</b>
2.1	Derivation from an Interacting Particle System . . . . .	3
2.2	The Aggregation–Diffusion Form . . . . .	3
2.3	Quadratic Interaction Kernel and Complexity Reduction . . . . .	3
<b>3</b>	<b>WANPM for the Stationary McKean–Vlasov Equation</b>	<b>4</b>
3.1	The Stationary Problem . . . . .	4
3.2	Weak Formulation . . . . .	4
3.3	Neural Parametrization . . . . .	5
3.4	Loss Function and Self-Consistency of the Mean Estimate . . . . .	5
3.5	Adversarial Training and Frequency Initialization . . . . .	5
3.6	Training Algorithm . . . . .	6

---

\*Department of Mathematics, Southern Methodist University, Dallas, TX, USA. [andrewhe@smu.edu](mailto:andrewhe@smu.edu), [cai@smu.edu](mailto:cai@smu.edu)

<b>4</b>	<b>Extension to the Time-Dependent Problem</b>	<b>7</b>
<b>5</b>	<b>Numerical Experiment</b>	<b>8</b>
5.1	Problem Setup: 1D Linear McKean–Vlasov . . . . .	8
5.2	Network Architecture and Training Details . . . . .	8
5.3	Results . . . . .	8
<b>6</b>	<b>Conclusion</b>	<b>8</b>

# 1 Introduction

The standard Fokker–Planck equation (FPE) governs the time evolution of the probability density  $\rho(t, \mathbf{x})$  of a stochastic process whose drift and diffusion coefficients are prescribed functions of  $(t, \mathbf{x})$ . A natural and physically important generalization arises when these coefficients depend on the evolving distribution  $\rho_t$  itself, yielding the McKean–Vlasov or mean-field Fokker–Planck equation:

$$\partial_t \rho(t, \mathbf{x}) = -\nabla_{\mathbf{x}} \cdot [b(\mathbf{x}, \rho_t) \rho(t, \mathbf{x})] + \frac{\sigma^2}{2} \Delta \rho(t, \mathbf{x}), \tag{1}$$

with initial condition  $\rho(0, \mathbf{x}) = \rho_0(\mathbf{x})$ . This class of equations appears in interacting particle systems and granular media [3], Curie–Weiss spin systems, stochastic flocking [4], mathematical finance and mean-field games [5], and the mean-field analysis of overparameterized neural networks [6].

The nonlinearity of (1) — the unknown  $\rho$  appears both as the evolved density and inside the convolution integral defining the drift — makes it significantly harder to solve than the standard FPE. Particle methods exploit the propagation of chaos phenomenon [2]: as  $N \rightarrow \infty$ , the empirical measure of  $N$  interacting particles converges to the solution of (1). However, particle methods suffer from statistical noise, require a large number of particles for accuracy, and do not naturally produce a functional representation of  $\rho$  that can be queried at arbitrary points.

Neural network methods for solving Fokker–Planck equations have been developed in several recent works [7, 8, 9, 10]. In [1], the Weak Adversarial Neural Pushforward Method (WANPM) was introduced, which learns a neural *pushforward map*  $F_{\mathfrak{g}} : \mathbb{R}^d \rightarrow \mathbb{R}^n$  that transforms samples from a simple base distribution into samples from the solution distribution, trained via an adversarial weak formulation with plane-wave test functions. WANPM avoids the need for explicit density representations, invertible architectures, or score estimation, and scales to high-dimensional problems.

The present paper extends WANPM to the McKean–Vlasov setting. The central finding is that for structurally simple interaction kernels — in particular, the quadratic (granular media) kernel  $W(\mathbf{x} - \mathbf{y}) = \frac{1}{2} \|\mathbf{x} - \mathbf{y}\|^2$  — the mean-field nonlinearity reduces to a sample mean of the primary training batch, and the standard WANPM training loop requires only minimal modification. We focus primarily on the stationary (time-independent) problem, developing both the mathematical formulation and the practical training considerations in detail, and briefly discuss the time-dependent extension.

The rest of this paper is organized as follows. Section 2 introduces the McKean–Vlasov equation and the quadratic interaction kernel. Section 3 develops WANPM for the stationary problem in detail, including the weak formulation, the loss function, the self-consistency of the mean-field estimate, the adversarial training algorithm, and practical training considerations. Section 4 briefly discusses the time-dependent extension. Section 5 presents the numerical benchmark, and Section 6 concludes.

## 2 The McKean–Vlasov Equation

### 2.1 Derivation from an Interacting Particle System

Consider  $N$  particles with positions  $X_i(t) \in \mathbb{R}^n$  obeying the coupled stochastic differential equations

$$dX_i = b\left(X_i, \frac{1}{N} \sum_{j=1}^N \delta_{X_j(t)}\right) dt + \sigma dW_i, \quad i = 1, \dots, N, \quad (2)$$

where  $W_i$  are independent standard Brownian motions and  $\delta_y$  denotes the Dirac measure at  $y$ . Each particle experiences a drift depending on the empirical measure of the entire population. By the propagation of chaos phenomenon [2], as  $N \rightarrow \infty$  the single-particle density satisfies the McKean–Vlasov equation (1).

### 2.2 The Aggregation–Diffusion Form

The most widely studied instance takes the drift as the superposition of a confinement force  $-\nabla V(\mathbf{x})$  and a pairwise interaction:

$$b(\mathbf{x}, \rho_t) = -\nabla V(\mathbf{x}) - \nabla(W * \rho_t)(\mathbf{x}) = -\nabla V(\mathbf{x}) - \int_{\mathbb{R}^n} \nabla W(\mathbf{x} - \mathbf{y}) \rho(t, \mathbf{y}) d\mathbf{y}, \quad (3)$$

with constant isotropic diffusion  $a(\mathbf{x}, \rho_t) = \sigma^2 I$ . Substituting (3) into (1) yields the aggregation–diffusion equation

$$\partial_t \rho = \nabla \cdot [(\nabla V)\rho] + \nabla \cdot [(\nabla W * \rho)\rho] + \frac{\sigma^2}{2} \Delta \rho. \quad (4)$$

The unknown  $\rho$  appears both as the evolved density and inside the convolution; this self-referential structure is the central mathematical difficulty.

### 2.3 Quadratic Interaction Kernel and Complexity Reduction

We focus on the quadratic (granular media) kernel  $W(\mathbf{x} - \mathbf{y}) = \frac{1}{2} \|\mathbf{x} - \mathbf{y}\|^2$ , for which a key simplification holds.

**Proposition 1** ([3]). *Let  $W(\mathbf{x} - \mathbf{y}) = \frac{1}{2} \|\mathbf{x} - \mathbf{y}\|^2$ . Then*

$$\int_{\mathbb{R}^n} \nabla W(\mathbf{x} - \mathbf{y}) \rho_t(\mathbf{y}) d\mathbf{y} = \mathbf{x} - m(t), \quad m(t) = \mathbb{E}_{\mathbf{y} \sim \rho_t}[\mathbf{y}]. \quad (5)$$

*Proof.* Direct computation:  $\nabla_{\mathbf{x}}W(\mathbf{x} - \mathbf{y}) = \mathbf{x} - \mathbf{y}$ , so  $\int(\mathbf{x} - \mathbf{y})\rho_t(\mathbf{y}) d\mathbf{y} = \mathbf{x} - m(t)$ .  $\square$

With confinement  $V(\mathbf{x}) = \frac{\theta}{2}\|\mathbf{x}\|^2$  and the quadratic kernel, the full drift simplifies to

$$b(\mathbf{x}, \rho_t) = -\theta\mathbf{x} - (\mathbf{x} - m(t)) = -(\theta + 1)\mathbf{x} + m(t) = -\lambda\mathbf{x} + m(t), \quad (6)$$

where  $\lambda := \theta + 1$  is the effective mean-reversion rate. The interaction integral reduces to the scalar  $m(t) = \mathbb{E}[\mathbf{x}]$ , which is the sample mean of the primary training batch — no secondary sampling is needed.

### 3 WANPM for the Stationary McKean–Vlasov Equation

#### 3.1 The Stationary Problem

Setting  $\partial_t\rho = 0$  in (1) yields the stationary McKean–Vlasov equation:

$$-\nabla \cdot [b(\mathbf{x}, \rho) \rho(\mathbf{x})] + \frac{\sigma^2}{2}\Delta\rho(\mathbf{x}) = 0, \quad \int_{\mathbb{R}^n} \rho(\mathbf{x}) d\mathbf{x} = 1. \quad (7)$$

This is a nonlinear eigenvalue problem: the operator acting on  $\rho$  depends on  $\rho$  itself through the convolution. For the quadratic kernel with  $V(\mathbf{x}) = \frac{\theta}{2}\|\mathbf{x}\|^2$ , the drift (6) gives  $b(\mathbf{x}, \rho) = -\lambda\mathbf{x} + m^*$  where  $m^* = \mathbb{E}_\rho[\mathbf{x}]$ . By symmetry of  $V$  and  $W$ , the unique stationary solution is  $\rho^* = \mathcal{N}(0, \frac{\sigma^2}{2\lambda}I)$  with  $m^* = 0$ , giving  $b(\mathbf{x}, \rho^*) = -\lambda\mathbf{x}$ .

The uniqueness follows from the strict convexity of the effective potential  $\Phi_\rho(\mathbf{x}) = V(\mathbf{x}) + (W * \rho)(\mathbf{x}) = \frac{\lambda}{2}\|\mathbf{x}\|^2$ , which rules out phase transitions; the self-consistent Boltzmann equation

$$\rho^*(\mathbf{x}) = Z^{-1} \exp\left(-\frac{2\Phi_{\rho^*}(\mathbf{x})}{\sigma^2}\right) \quad (8)$$

has a unique Gaussian fixed point.

#### 3.2 Weak Formulation

Multiplying (7) by a smooth test function  $f(\mathbf{x})$  and integrating by parts gives the stationary weak form:

$$\mathbb{E}_{\mathbf{x} \sim \rho}[\mathcal{L}[\rho] f(\mathbf{x})] = 0 \quad \forall f \in C_c^\infty(\mathbb{R}^n), \quad (9)$$

where the generator of the self-consistent diffusion is

$$\mathcal{L}[\rho] f(\mathbf{x}) = b(\mathbf{x}, \rho) \cdot \nabla f(\mathbf{x}) + \frac{\sigma^2}{2}\Delta f(\mathbf{x}). \quad (10)$$

We choose plane-wave test functions  $f^{(k)}(\mathbf{x}) = \sin(\mathbf{w}^{(k)} \cdot \mathbf{x} + b^{(k)})$ , for which all derivatives are available analytically:

$$\nabla f^{(k)}(\mathbf{x}) = \mathbf{w}^{(k)} \cos(\mathbf{w}^{(k)} \cdot \mathbf{x} + b^{(k)}), \quad \Delta f^{(k)}(\mathbf{x}) = -\|\mathbf{w}^{(k)}\|^2 \sin(\mathbf{w}^{(k)} \cdot \mathbf{x} + b^{(k)}). \quad (11)$$

Substituting (6) and (11) into (10) gives, for the quadratic kernel:

$$\mathcal{L}[\rho] f^{(k)}(\mathbf{x}) = (-\lambda\mathbf{x} + m^*) \cdot \mathbf{w}^{(k)} \cos(\mathbf{w}^{(k)} \cdot \mathbf{x} + b^{(k)}) - \frac{\sigma^2}{2}\|\mathbf{w}^{(k)}\|^2 \sin(\mathbf{w}^{(k)} \cdot \mathbf{x} + b^{(k)}). \quad (12)$$

The mean  $m^* = \mathbb{E}_\rho[\mathbf{x}]$  is the only quantity that depends on  $\rho$  in a nonlinear way.

### 3.3 Neural Parametrization

**Pushforward network.** We parametrize the stationary distribution  $\rho^*$  implicitly via a neural pushforward map  $F_{\boldsymbol{\vartheta}} : \mathbb{R}^d \rightarrow \mathbb{R}^n$ , where  $d$  is the dimension of the base distribution (not necessarily equal to  $n$ ). If  $\mathbf{r} \sim \pi_{\text{base}}$ , then  $\mathbf{x} = F_{\boldsymbol{\vartheta}}(\mathbf{r})$  is a sample from the learned distribution  $\rho_{\boldsymbol{\vartheta}}$ . The pushforward parametrization naturally enforces the normalization constraint and can represent distributions without a classical density. In the stationary setting, there is no time variable and no initial condition, so  $F_{\boldsymbol{\vartheta}}$  takes only the base noise  $\mathbf{r}$  as input.

**Test functions.** We use  $K$  plane-wave test functions with learnable frequency vectors  $\mathbf{w}^{(k)} \in \mathbb{R}^n$  and bias terms  $b^{(k)} \in \mathbb{R}$ , organized into parameter sets  $\boldsymbol{\eta}^{(k)} = \{\mathbf{w}^{(k)}, b^{(k)}\}_{k=1}^K$ .

### 3.4 Loss Function and Self-Consistency of the Mean Estimate

The training objective is the adversarial squared weak residual:

$$\mathcal{L}_{\text{total}}[\boldsymbol{\vartheta}, \boldsymbol{\eta}] = \frac{1}{K} \sum_{k=1}^K \left[ \frac{1}{M} \sum_{m=1}^M \mathcal{L}[\rho_{\boldsymbol{\vartheta}}] f^{(k)}(\mathbf{x}^{(m)}) \right]^2, \quad (13)$$

where  $\{\mathbf{x}^{(m)} = F_{\boldsymbol{\vartheta}}(\mathbf{r}^{(m)})\}_{m=1}^M$  is a batch of pushed samples and  $m^*$  is approximated by the batch mean  $\hat{m} = \frac{1}{M} \sum_m \mathbf{x}^{(m)}$ .

A critical subtlety concerns whether to detach  $\hat{m}$  from the gradient graph. If  $\hat{m}$  is detached (i.e. treated as a fixed constant when computing gradients with respect to  $\boldsymbol{\vartheta}$ ), the gradient of (13) does not encode the self-consistency constraint  $m^* = \mathbb{E}_{\rho_{\boldsymbol{\vartheta}}}[\mathbf{x}]$ . Consequently, the network may converge to distributions that have the correct mean and variance but wrong shape, since any distribution with the appropriate moments will satisfy the weak residual (9) with  $m^*$  treated as fixed.

Instead,  $\hat{m}$  must be computed from the same batch as the residual, with gradient flowing through it:

$$\hat{m} = \frac{1}{M} \sum_{m=1}^M F_{\boldsymbol{\vartheta}}(\mathbf{r}^{(m)}), \quad \mathbf{r}^{(m)} \sim \pi_{\text{base}}. \quad (14)$$

This allows the gradient  $\partial \hat{m} / \partial \boldsymbol{\vartheta}$  to contribute to the total gradient, coupling the mean estimate to the distribution and enforcing self-consistency through the optimization dynamics.

### 3.5 Adversarial Training and Frequency Initialization

The min-max optimization problem is:

$$\min_{\boldsymbol{\vartheta}} \max_{\boldsymbol{\eta}} \mathcal{L}_{\text{total}}[\boldsymbol{\vartheta}, \boldsymbol{\eta}]. \quad (15)$$

The generator (pushforward network) takes gradient descent steps to minimize  $\mathcal{L}_{\text{total}}$ , while the adversary (test function parameters) takes gradient ascent steps to maximize it.

A second critical subtlety concerns the initialization scale of the frequency vectors  $\mathbf{w}^{(k)}$ . For the quadratic kernel, the two-point distribution  $\rho_{\text{two}} = \frac{1}{2}\delta_{-a} + \frac{1}{2}\delta_{+a}$  with  $a = \sigma/\sqrt{2\lambda}$  has

the same mean and variance as the true stationary Gaussian, and therefore satisfies the weak residual approximately when test function frequencies are small. One can verify analytically that the residual under  $\rho_{\text{two}}$  at a plane-wave test function with frequency  $w$  and bias  $b$  is:

$$R_{\text{two}}^{(k)} = \sin(wa) \left[ \lambda a w \sin(b) - \frac{\sigma^2 w^2}{2} \cos(b) \right], \quad (16)$$

while the exact Gaussian gives  $R_{\text{Gaussian}}^{(k)} = 0$  for all  $(w, b)$ . For small  $w$  (specifically when  $wa \ll 1$ ), the factor  $\sin(wa) \approx wa$  is small, and  $|R_{\text{two}}^{(k)}|$  is comparably small to  $|R_{\text{Gaussian}}^{(k)}|$ . In this regime, the two-point distribution can achieve a lower loss value than the exact Gaussian. Table 1 confirms this numerically.

Table 1: Loss values for the two-point distribution and exact Gaussian at different test function frequency scales, with  $\theta = 1$ ,  $\sigma = 1$ ,  $\lambda = 2$ ,  $a = 0.5$ . Results averaged over  $K = 1000$  random test functions and  $M = 50,000$  samples.

Frequency scale	Two-point loss	Gaussian loss
$\ \mathbf{w}\  \sim 0.3$ (small)	$7.1 \times 10^{-6}$	$1.6 \times 10^{-5}$
$\ \mathbf{w}\  \sim 2.0$ (large)	$5.0 \times 10^0$	$1.1 \times 10^{-3}$

When frequencies are initialized small (scale 0.3), the two-point distribution achieves a lower loss than the Gaussian, and the generator converges to this spurious solution. When frequencies are initialized at scale 2.0, the two-point distribution has a catastrophically large loss ( $\approx 5$ ), while the Gaussian retains a small loss ( $\approx 10^{-3}$ ), so the adversary correctly penalizes the wrong shape and the generator is driven toward the true solution.

### 3.6 Training Algorithm

The complete training procedure is summarized in Algorithm 1.

---

#### Algorithm 1 WANPM for the Stationary McKean–Vlasov Equation

---

**Require:** Pushforward net  $F_{\vartheta}$ , test functions  $\{f^{(k)}\}_{k=1}^K$  with  $\mathbf{w}^{(k)}$  initialized at scale 2.0, batch size  $M$ , learning rates  $\eta_{\text{gen}}$ ,  $\eta_{\text{test}}$ .

- 1: **for** each training epoch **do**
  - 2:   Sample  $\{\mathbf{r}^{(m)}\}_{m=1}^M \sim \pi_{\text{base}}$
  - 3:   Compute pushed samples  $\mathbf{x}^{(m)} = F_{\vartheta}(\mathbf{r}^{(m)})$
  - 4:   Compute batch mean  $\hat{m} = \frac{1}{M} \sum_m \mathbf{x}^{(m)}$  *(gradient flows through  $\hat{m}$ )*
  - 5:   Evaluate  $\mathcal{L}[\rho]f^{(k)}(\mathbf{x}^{(m)})$  using (12) with  $m^* \leftarrow \hat{m}$
  - 6:   Compute residuals  $R^{(k)} = \frac{1}{M} \sum_m \mathcal{L}[\rho]f^{(k)}(\mathbf{x}^{(m)})$
  - 7:   Compute loss  $\mathcal{L}_{\text{total}} = \frac{1}{K} \sum_k (R^{(k)})^2$
  - 8:   **Generator step:**  $\vartheta \leftarrow \vartheta - \eta_{\text{gen}} \nabla_{\vartheta} \mathcal{L}_{\text{total}}$
  - 9:   **if** epoch mod 2 = 0 **then**
  - 10:     **Adversary step:**  $\eta \leftarrow \eta + \eta_{\text{test}} \nabla_{\eta} \mathcal{L}_{\text{total}}$
  - 11:   **end if**
  - 12: **end for**
-

**Remark on Remark 2 of the companion notes.** The stationary self-consistent equation (8) suggests an outer fixed-point (Picard) iteration. WANPM avoids this: the adversarial training simultaneously drives the pushforward toward a distribution satisfying (9), with the mean-field drift updated at each step from the current batch. Provided gradient flow through  $\hat{m}$  is maintained, this implicit self-consistency is a key algorithmic advantage.

## 4 Extension to the Time-Dependent Problem

For the time-dependent McKean–Vlasov equation (1), WANPM employs the time-parameterized pushforward map

$$F_{\vartheta}(t, \mathbf{x}_0, \mathbf{r}) = \mathbf{x}_0 + \sqrt{t} \tilde{F}_{\vartheta}(t, \mathbf{x}_0, \mathbf{r}), \quad (17)$$

where  $\mathbf{x}_0 \sim \rho_0$  and  $\mathbf{r} \sim \pi_{\text{base}}$ . The  $\sqrt{t}$  factor enforces  $F_{\vartheta}(0, \mathbf{x}_0, \mathbf{r}) = \mathbf{x}_0$  by construction, automatically satisfying the initial condition. The resulting three-term weak form,

$$\mathbb{E}_{\rho_{(T, \cdot)}}[f(T, \cdot)] - \mathbb{E}_{\rho_0}[f(0, \cdot)] - \int_0^T \mathbb{E}_{\mathbf{x} \sim \rho(t, \cdot)} \left[ \frac{\partial f}{\partial t} + \mathcal{L}[\rho_t]f(t, \mathbf{x}) \right] dt = 0, \quad (18)$$

is approximated by Monte Carlo, as in [1].

The key additional difficulty in the McKean–Vlasov setting is the estimation of  $m(t) = \mathbb{E}_{\rho_t}[\mathbf{x}]$  for each time point sampled in the interior term. A naive approach—computing the mean over all  $M$  interior samples at  $M$  different random times—produces a time-averaged constant  $\hat{m} \approx \frac{1}{T} \int_0^T m(t) dt$ , which biases the drift and prevents the learned mean from decaying correctly.

The correct approach uses a *tensor-product sampling structure*: draw  $N_T$  fixed quadrature points  $\{t_i\}_{i=1}^{N_T}$  on  $(0, T]$  and, at each  $t_i$ , draw  $M_{\text{per}}$  independent base samples  $(\mathbf{x}_0^{(j)}, \mathbf{r}^{(j)})_{j=1}^{M_{\text{per}}}$ . Then

$$\hat{m}(t_i) = \frac{1}{M_{\text{per}}} \sum_{j=1}^{M_{\text{per}}} F_{\vartheta}(t_i, \mathbf{x}_0^{(j)}, \mathbf{r}^{(j)}) \quad (19)$$

is a valid unbiased estimate of  $m(t_i)$ , and the interior term is approximated by the quadrature sum

$$\hat{E}^{(k)} = \frac{T}{N_T} \sum_{i=1}^{N_T} \frac{1}{M_{\text{per}}} \sum_{j=1}^{M_{\text{per}}} [\partial_t f^{(k)} + \mathcal{L}[\rho_{t_i}]f^{(k)}] \left( t_i, F_{\vartheta}(t_i, \mathbf{x}_0^{(j)}, \mathbf{r}^{(j)}) \right). \quad (20)$$

The total number of forward passes  $N_T \times M_{\text{per}}$  matches the standard WANPM interior batch size, so there is no additional computational cost. The same base samples  $(\mathbf{x}_0^{(j)}, \mathbf{r}^{(j)})$  are reused across all time points  $t_i$ , which is valid because the pushforward at different times evaluates  $F_{\vartheta}(t_i, \mathbf{x}_0^{(j)}, \mathbf{r}^{(j)})$  — a deterministic function of  $(t_i, \mathbf{x}_0^{(j)}, \mathbf{r}^{(j)})$  — producing independent samples from  $\rho_{t_i}$  for each  $i$  (since  $t_i$  differs). The fixed quadrature nodes ensure that the mean estimate  $\hat{m}(t_i)$  correctly reflects the distribution at  $t_i$  rather than an average over a range of times.

## 5 Numerical Experiment

### 5.1 Problem Setup: 1D Linear McKean–Vlasov

We consider the one-dimensional stationary McKean–Vlasov equation with  $n = 1$ ,  $\theta = 1$ ,  $\sigma = 1$ , so that  $\lambda = \theta + 1 = 2$  and the exact stationary solution is

$$\rho^* = \mathcal{N}\left(0, \frac{\sigma^2}{2\lambda}\right) = \mathcal{N}(0, 0.25). \quad (21)$$

The base distribution is  $\pi_{\text{base}} = \mathcal{U}[0, 1)$ , mapping from a bounded uniform distribution to an unbounded Gaussian target, which tests the representational capacity of the pushforward network.

### 5.2 Network Architecture and Training Details

The pushforward network  $F_{\mathcal{G}} : \mathbb{R}^1 \rightarrow \mathbb{R}^1$  has architecture  $(1, 10, 10, 1)$  with Tanh activations, matching the architecture used in [1] for the one-dimensional FPE benchmark. The test function ensemble consists of  $K = 1000$  plane-wave functions with frequencies  $\mathbf{w}^{(k)}$  initialized at scale 2.0 (i.e.  $\mathbf{w}^{(k)} \sim \mathcal{N}(0, 4)$ ) and biases  $b^{(k)} \sim \mathcal{N}(0, 4\pi^2)$ . The batch size is  $M = 1000$ . Training runs for 5000 epochs with generator learning rate  $\eta_{\text{gen}} = 10^{-3}$  (Adam optimizer) and adversary learning rate  $\eta_{\text{test}} = 10^{-2}$  (SGD), with one adversary update every two generator steps. The batch mean  $\hat{m}$  is computed from the same batch as the residual with full gradient flow, as described in Section 3.

### 5.3 Results

Figures 1 and 2 show the learned stationary distribution, the Q-Q plot, and the training loss convergence.

The learned distribution agrees closely with the exact Gaussian. The Q-Q plot is nearly linear throughout the quantile range, indicating accurate distributional agreement including the tails. The numerical statistics of the learned distribution are:

$$\hat{\mu} = -0.000354 \approx 0, \quad \hat{\sigma} = 0.491973 \approx 0.5, \quad \hat{\Sigma} = 0.242038 \approx 0.25,$$

with absolute errors  $|\hat{\mu} - \mu^*| = 3.5 \times 10^{-4}$ ,  $|\hat{\sigma} - \sigma^*| = 8.0 \times 10^{-3}$ , and  $|\hat{\Sigma} - \Sigma^*| = 8.0 \times 10^{-3}$ . The training loss converges from an initial value of approximately 6 to a final value of  $9.6 \times 10^{-6}$  in 5000 epochs, requiring approximately 1.1 minutes on a single GPU.

## 6 Conclusion

We have developed the Weak Adversarial Neural Pushforward Method for the McKean–Vlasov mean-field Fokker–Planck equation, focusing on the stationary problem. The key findings are:

1D Stationary McKean-Vlasov: WANPM vs Exact Gaussian

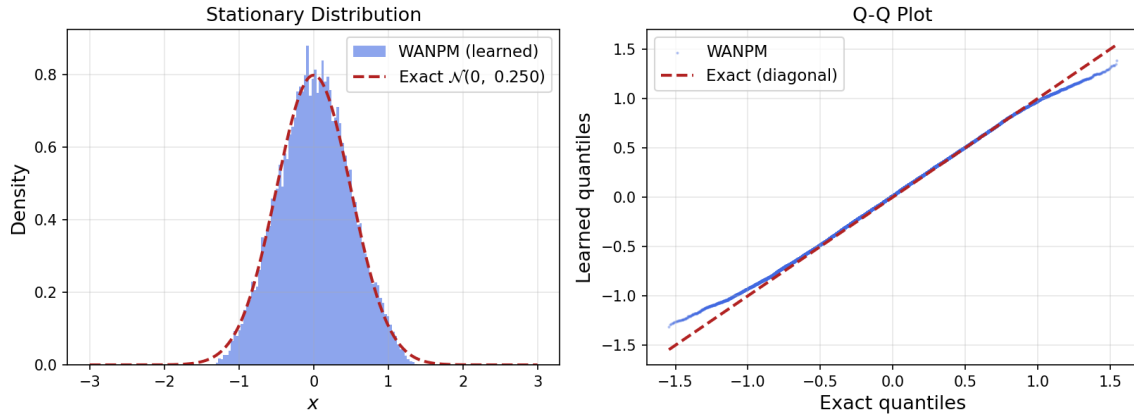


Figure 1: Learned stationary distribution (histogram) vs. exact  $\mathcal{N}(0, 0.25)$  (dashed red). Left panel: density comparison. Right panel: Q-Q plot confirming distributional agreement throughout the quantile range. Parameters:  $\theta = 1$ ,  $\sigma = 1$ , base distribution  $\mathcal{U}[0, 1)$ , network architecture  $(1, 10, 10, 1)$ .



Figure 2: Training loss convergence. The loss decreases steadily over five orders of magnitude from an initial value near  $10^1$  to a final value of  $9.6 \times 10^{-6}$ , confirming stable adversarial training dynamics.

- For the quadratic interaction kernel, the mean-field nonlinearity reduces to the sample mean of the primary training batch, requiring no secondary sampling and no modification to the pushforward architecture.
- The batch mean estimate must be computed from the same batch as the residual, with gradient flowing through it. Detaching the mean estimate breaks the self-consistency coupling  $m^* = \mathbb{E}_\rho[\mathbf{x}]$  and allows spurious non-Gaussian solutions with correct mean and variance but wrong shape.
- The initialization scale of adversarial test function frequencies is critical. Small initial frequencies allow the two-point distribution (which has the same mean and variance as the exact Gaussian) to achieve a lower loss than the true solution. Initializing frequencies at scale 2.0 ensures that the adversary can detect and penalize this spurious solution from the start of training.
- For the time-dependent McKean–Vlasov problem, a tensor-product sampling structure over space and time — fixed quadrature nodes in  $t$  and independent Monte Carlo draws in  $(\mathbf{x}_0, \mathbf{r})$  shared across all time nodes — is required to obtain valid per-time mean-field estimates without bias.

The quadratic (granular media) kernel is the natural first implementation target due to its zero overhead, exact Gaussian benchmark, and rich physical literature. Natural extensions include higher-degree polynomial kernels (whose interaction integrals reduce to batch moments), separable kernels (whose interaction integrals reduce to  $L$  scalar expectations), and higher-dimensional stationary and time-dependent problems. The Keller–Segel kernel  $W(\mathbf{x}) = -\log \|\mathbf{x}\|$  requires a secondary batch for the interaction integral and represents the most challenging case within this framework.

## References

- [1] A. Q. He and W. Cai, *Neural Pushforward Samplers for Transient Distributions from Fokker–Planck Equations with Weak Adversarial Training*, arXiv:2509.14575, 2025.
- [2] A. S. Sznitman, *Topics in propagation of chaos*, in *École d’Été de Probabilités de Saint-Flour XIX—1989*, Lecture Notes in Math. 1464, Springer, Berlin, 1991, pp. 165–251.
- [3] R. J. McCann, *A convexity principle for interacting gases*, *Adv. Math.* **128** (1997), 153–179.
- [4] S.-Y. Ha and E. Tadmor, *From particle to kinetic and hydrodynamic descriptions of flocking*, *Kinet. Relat. Models* **1** (2008), 415–435.
- [5] R. Carmona and F. Delarue, *Probabilistic Theory of Mean Field Games with Applications I*, Springer, Cham, 2018.
- [6] S. Mei, A. Montanari, and P.-M. Nguyen, *A mean field view of the landscape of two-layer neural networks*, *Proc. Natl. Acad. Sci. USA* **115** (2018), E7665–E7671.

- [7] Y. Xu, H. Zhang, Y. Li, K. Zhou, Q. Liu, and J. Kurths, *Solving Fokker–Planck equation using deep learning*, *Chaos* **30** (2020), 013133.
- [8] S. Liu, W. Li, S. Osher, and W. Yin, *Neural Parametric Fokker–Planck Equations*, arXiv:2002.11309, 2022.
- [9] W. E, J. Han, and Q. Li, *A mean-field optimal control formulation of deep learning*, *Res. Math. Sci.* **6** (2019), 10.
- [10] J. Zhai, M. Dobson, and Y. Li, *A deep learning method for solving Fokker–Planck equations*, in *Proceedings of the 2nd Mathematical and Scientific Machine Learning Conference*, *Proc. Mach. Learn. Res.* **145**, 2022, pp. 568–597.